Structure of Cholesterol in Lipid Rafts

Laura Toppozini,[1] Sebastian Meinhardt,[2] Clare L. Armstrong,[1] Zahra Yamani,[3] Norbert Kučerka,[3,4] Friederike Schmid,[2,†] and Maikel C. Rheinstädter[1,3,*]

[1]Department of Physics and Astronomy, McMaster University, Hamilton, Ontario, L8S 4M1, Canada
[2]KOMET 331, Institute of Physics, Johannes Gutenberg-Universität Mainz, 55099 Mainz, Germany
[3]Canadian Neutron Beam Centre, Chalk River, Ontario, K0J 1J0, Canada
[4]Faculty of Pharmacy, Comenius University, 832 32 Bratislava, Slovakia

(Received 17 March 2014; published 25 November 2014)

Rafts, or functional domains, are transient nano-or mesoscopic structures in the plasma membrane and are thought to be essential for many cellular processes such as signal transduction, adhesion, trafficking, and lipid or protein sorting. Observations of these membrane heterogeneities have proven challenging, as they are thought to be both small and short lived. With a combination of coarse-grained molecular dynamics simulations and neutron diffraction using deuterium labeled cholesterol molecules, we observe raftlike structures and determine the ordering of the cholesterol molecules in binary cholesterol-containing lipid membranes. From coarse-grained computer simulations, heterogenous membranes structures were observed and characterized as small, ordered domains. Neutron diffraction was used to study the lateral structure of the cholesterol molecules. We find pairs of strongly bound cholesterol molecules in the liquid-disordered phase, in accordance with the umbrella model. Bragg peaks corresponding to ordering of the cholesterol molecules in the raftlike structures were observed and indexed by two different structures: a monoclinic structure of ordered cholesterol pairs of alternating direction in equilibrium with cholesterol plaques, i.e., triclinic cholesterol bilayers.

DOI: 10.1103/PhysRevLett.113.228101 PACS numbers: 87.16.dt, 83.85.Hf, 87.15.ap

The liquid-ordered (l_o) phase of membranes in the presence of cholesterol was brought to the attention of the life science community in 1997 when Simons and Ikonen [1] proposed the existence of so-called rafts in biological membranes. Rafts were thought to be small, molecularly organized units, providing local structure in fluid biological membranes and hence furnishing platforms for specific biological functions [1–10]. These rafts were supposed to be enriched in cholesterol making them more ordered, thicker and, thus, appropriate anchoring places for certain acylated and hydrophobically matched integral membrane proteins. The high levels of cholesterol in these rafts led to the proposal that rafts are local manifestations of the l_o phase, although in most cases the nature of the lipid ordering and the phase state were not established in cells, nor in most model membrane studies [10–12].

Rafts are generally interpreted as self-assembled clusters floating around in an otherwise structureless liquid membrane. However, early work in the physical chemistry of lipid bilayers pointed to the possibility of dynamic heterogeneity [13–16] in thermodynamic one-phase regions of binary systems. The sources of dynamic heterogeneity are cooperative molecular interactions and thermal fluctuations that lead to density and compositional fluctuations in space and time.

A number of ternary phase diagrams have been determined for systems involving cholesterol and two different lipid species. Usually these systems contain a lipid species with a high melting point, such as a long-chain saturated phospholipid or sphingolipid, and a lipid species with a low melting point, such as an unsaturated phospholipid [17], resulting in the observations of micrometer-sized, thermodynamically stable domains [4,18–21]. Much less work has been done on cholesterol-lipid binary mixtures, which although seemingly simpler, have proven to be more difficult to study. Evidence for a heterogeneous structure of the l_o phase, similar to a microemulsion, with ordered lipid nanodomains in equilibrium with a disordered membrane was recently supported both by theory and experiment. The computational work by Meinhardt, Vink, and Schmid [22] and Sodt *et al.* [23] and the experimental papers by Armstrong *et al.* [24–26] using neutron scattering were conducted using binary DPPC/cholesterol and dimyristoylphosphocholine (DMPC)/cholesterol systems.

We combined coarse-grained molecular dynamics (MD) simulations including 20 000 lipid-cholesterol molecules with neutron diffraction using deuterium labeled cholesterol molecules to study the cholesterol structure in the liquid-ordered phase of dipalmitoylphosphatidylcholine (DPPC) bilayers. The simulations present evidence for a heterogenous membrane structure at 17 and 60 mol% cholesterol and the formation of small, transient domains enriched in cholesterol. The molecular structure of the cholesterol molecules within these domains was determined by neutron diffraction at 32.5 mol% cholesterol. Three structures were observed: (1) a fluidlike structure with strongly bound pairs of cholesterol molecules as manifestation of the liquid-disordered (l_d) phase; (2) a highly ordered lipid-cholesterol phase where the lipid-cholesterol

complexes condense in a monoclinic structure, in accordance with the umbrella model; and (3) triclinic cholesterol plaques, i.e., cholesterol bilayers coexisting with the lamellar lipid membranes.

The simulations use a simple coarse-grained lipid model [27] that reproduces the main phases of DPPC bilayers including the nanostructured ripple phase $P_{\beta'}$ [27] and has similar elastic properties in the fluid phase [28]. In this model, lipids are represented by short linear chains of beads, with a "head bead" and several "tail beads" [Fig. 1(a)], which are surrounded by a structureless solvent. The model was recently extended to binary lipid-cholesterol mixtures. The cholesterol molecules are modeled shorter and stiffer than DPPC, and they have an affinity to phospholipid molecules, reflecting the observation that sterols in bilayers tend to be solubilized by lipids [29]. In our previous work, we have reported on the behavior of mixed bilayers with low cholesterol content [22]. Locally, phase separation was observed between an l_o and an l_d phase. On large scales, however, the system assumes a two-dimensional microemulsion-type state, where nanometer-sized cholesterol-rich domains are embedded in an l_d environment. These domains are stabilized by a coupling between monolayer curvature and local ordering [22], suggesting that raft formation is closely related to the formation of ripples in one-component membranes. In the following, we will discuss the behavior of our model membranes at larger cholesterol concentrations and discuss the implications for experiments.

The simulations were done at constant pressure, constant temperature, and constant zero surface tension in a semi-grandcanonical ensemble where lipids and cholesterol molecules can switch their identities. The cholesterol content is thus driven by a chemical potential parameter μ. Simulation results are given in units of $\sigma \approx 6$ Å [28] and the thermal energy k_BT. Typical equilibrated simulation snapshots (side view and top view) are shown in Figs. 1(b) and 1(c). At low cholesterol concentration ($\mu = 8.5k_BT$), one observes small rafts as discussed earlier. At higher cholesterol concentration (lower μ), the cholesterol-rich rafts grow and gradually fill up the system, but they still remain separated by narrow cholesterol-poor "trenches." The side view shows that these trenches have the structure of line defects where opposing monolayers are connected. Such line defects are also structural elements of the ripple phase in one-component bilayers [30,31].

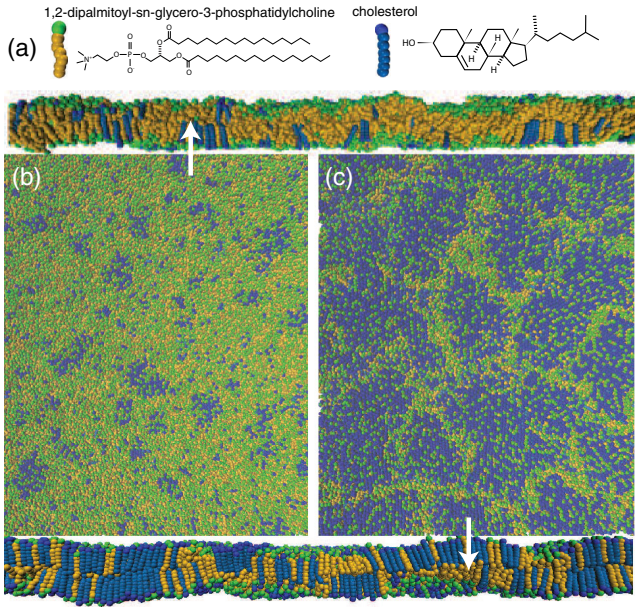

FIG. 1 (color online). (a) Schematic representation of DPPC and cholesterol molecules used in the simulations. (b) Snapshot of the simulation at $\mu = 8.5k_BT$, resulting in a cholesterol concentration of ≈17 mol%. (c) Snapshot of the simulation at $\mu = 7.8k_BT$ resulting in a cholesterol concentration of ≈60 mol%.

With increasing cholesterol concentration, the structure of the rafts changes qualitatively. This is demonstrated in Fig. 2(a), which shows that the cholesterol concentration inside rafts remains constant (around 25%) for a range of chemical potentials $\mu > 8.5k_BT$, but then increases rapidly at $\mu \leq 8k_BT$. Along with this concentration increase, the peaks in the lateral structure factor of cholesterol head groups in Fig. 2(b) become more pronounced, indicating a substantial increase in molecular order. We should note that the coarse-grained model used in the simulations is not suitable for studying details of the molecular arrangement inside the ordered structures. However, one can analyze the transition between states with high and low μ by analyzing the distribution of local cholesterol densities [Fig. 2(a), inset]. At high μ, the histogram has a maximum at cholesterol density c close to zero and decays for higher c with a broad tail that reflects the contribution of the rafts. At low μ, it exhibits a marked maximum at $c \approx 1\sigma^{-2}$, corresponding to bilayer regions consisting purely of cholesterol. In the intermediate regime, corresponding to the situation shown in Fig. 1(c), the histogram of cholesterol densities features two broad peaks around $c \approx 0.4\sigma^{-2}$ and $c \approx 0.7\sigma^{-2}$. In this regime, almost pure cholesterol plaques coexist with regions having cholesterol

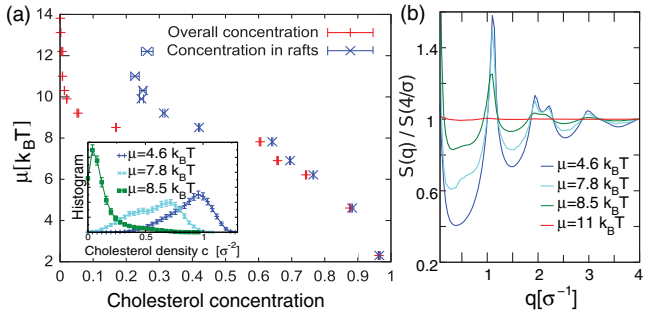

FIG. 2 (color online). (a) Total cholesterol concentration and cholesterol concentration inside rafts for different chemical potential μ. Inset shows a histogram of local cholesterol densities, taken using squares of area $25\sigma^2 \approx 9$ nm^2. (b) Radially averaged two-dimensional lateral structure factor of cholesterol head groups for different μ as indicated. The level of molecular order increases with decreasing μ, i.e., increasing cholesterol concentration.

compositions that are close to those of rafts in cholesterol-poor membranes [high μ limit in Fig. 2(a)].

The experimental observation of the l_o phase in a cholesterol-lipid binary mixture was initially reported by Vist and Davis [32]. The quantitative determination of binary lipid-cholesterol phase diagrams has remained elusive. In phospholipid membranes, most studies report the l_o phase at cholesterol concentrations of more than 30 mol% [17]. The formation of cholesterol plaques, phase-separated cholesterol bilayers coexisting with the membrane, was reported to occur at ≈37.5 mol% cholesterol in model lipid membranes [33]. That leaves a relatively small range of cholesterol concentrations in the experiment (between about 30 and 37.5 mol%), where the l_o phase can be studied. Phase separation may be driven in experiments by certain boundary conditions, not present in computer simulations. The simulations in Fig. 2 can, therefore, access a much larger range of cholesterol concentrations and by studying concentrations slightly lower and higher than the experimentally accessible range, the corresponding structures could be emphasized in the computer model.

We used neutron diffraction to measure the lateral cholesterol structure in DPPC bilayers containing 32.5 mol% at $T = 50\,^{\circ}\mathrm{C}$ and a D_2O relative humidity of ≈100%, ensuring full hydration of the membranes. Deuterium labeled cholesterol (d7) was used such that the experiment was sensitive to the arrangements of the cholesterol molecules. Schematics of the two molecules are shown in Fig. 3(a). Highly oriented, solid supported membrane stacks on silicon wafers were prepared, as detailed in the Supplemental Material [34]. The sample was aligned in the neutron beam such that the scattering vector, $\vec{Q}$, was placed in the plane of the membranes [Fig. 3(b)]. This in-plane component of the scattering vector is referred to as $q_{\|}$.

Two setups were used: a conventional high-energy and momentum resolution setup using a neutron wavelength of $\lambda = 2.37$ Å and a low-energy and momentum resolution setup with smaller wavelengths of $\lambda = 1.44$ and 1.48 Å. The latter setup was reported to efficiently integrate over small structures and provide a high spatial resolution capable of detecting small structures and weak signals [12,25,46]. The two setups could be readily switched during the experiment by changing the incoming neutron wavelength, λ, without altering the state of the membrane sample. Data taken using the conventional setup are shown in Fig. 3(c) and display a diffraction pattern with broad peaks, typical of a fluidlike structure.

Peaks T_1, T_2, and T_3 in Fig. 3(c) correspond to the hexagonal arrangement of the lipid tails with a unit cell of $a_{\mathrm{lipid}-l_d} = b_{\mathrm{lipid}-l_d} = 5.58$ Å and $\gamma = 120°$, in agreement with Armstrong *et al.* [25]. By calculating the (coherent) scattering contributions (Table S3 [34]), cholesterol and lipid molecules contribute almost equally to the scattering in the l_d phase such that the corresponding signals are observed simultaneously in Fig. 3(c). Peak H agrees well with an

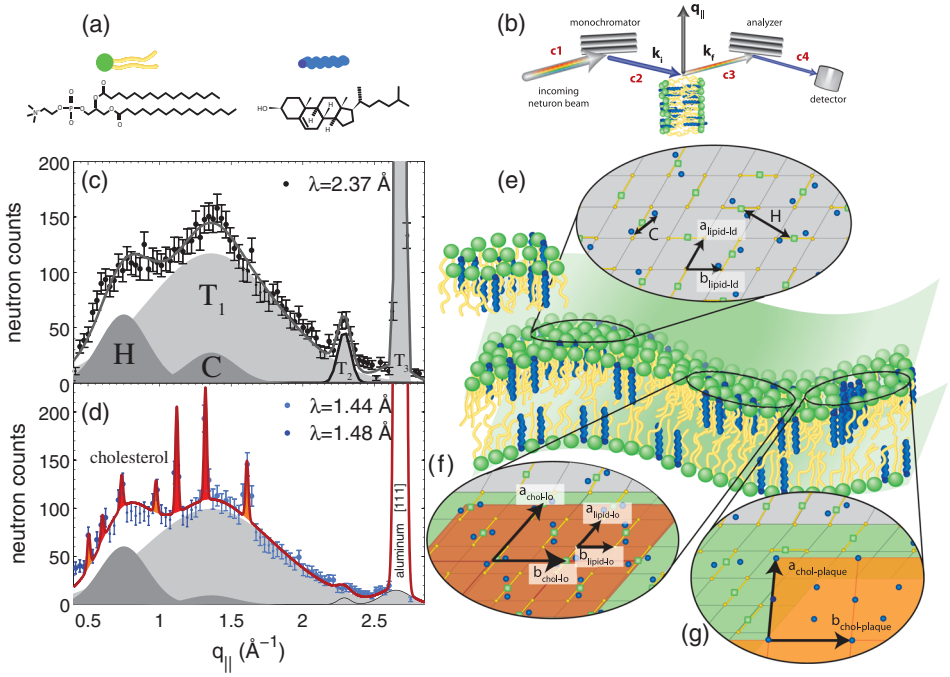

FIG. 3 (color online). (a) Schematics of DPPC and (deuterated) cholesterol molecules. (b) Sketch of the scattering geometry. $q_{\|}$ denotes the in-plane component of the scattering vector. (c) Diffraction measured at $\lambda = 2.37$ Å showing broad, fluidlike peaks. (d) Data measured at $\lambda = 1.44$ and 1.48 Å. Several pronounced Bragg peaks are observed in addition to the broad peaks in (a). (e) Illustration of the different molecular structures: pairs of cholesterol molecules in the liquid-disordered regions of the membrane in equilibrium with highly ordered cholesterol structures such as the umbrella structure (f) and cholesterol plaques (g). An aluminum Bragg peak due to the windows of the humidity chamber and the sample holder is present at $q_{\|} = 2.68$ Å^{-1}. Aluminum forms a face-centered cubic lattice with lattice parameter $a = 4.04941$ Å [45].

average nearest neighbor head group-head group distance of ≈8.4 Å. Peak C only occurs in the presence of deuterated cholesterol molecules. It was, therefore, assigned to a nearest neighbor distance of ≈4.6 Å (±0.5 Å) of cholesterol molecules in the l_d phase, i.e., to pairs of strongly bound cholesterol molecules, as shown in Fig. 3(e). Details of the fitting procedure are given in the Supplemental Material [34].

Several pronounced Bragg peaks are observed at neutron wavelengths of $\lambda = 1.44$ and 1.48 Å in Fig. 3(d) in addition to the broad correlation peaks. Because of the high cholesterol concentration in l_o-type structures and plaques and the scattering lengths of DPPC and d-cholesterol molecules, the corresponding coherent scattering signal in Fig. 3(d) is dominated by the deuterated cholesterol molecules. As listed in Table I, the peak pattern is well described by a superposition of two 2-dimensional structures: a monoclinic unit cell with lattice parameters $a_{\text{chol-lo}} = b_{\text{chol-lo}} = 11$ Å and $\gamma = 131°$ and a triclinic unit cell with $a_{\text{chol-plaque}} = b_{\text{chol-plaque}} = 12.8$ Å and $\gamma = 95°$ (the values for α and β could not be determined from the measurements but were taken from [33,47] to be $\alpha = 91.9°$ and $\beta = 98.1°$).

The lipid structure in the l_o-type structures in binary DPPC/32.5 mol% cholesterol bilayers was recently reported by Armstrong *et al.* from neutron diffraction using deuterium labeled lipid molecules [25]. The lipid tails were found in an ordered, gel-like phase organized in a monoclinic unit cell with $a_{\text{lipid-lo}} = b_{\text{lipid-lo}} = 5.2$ Å and $\gamma = 130.7°$, as shown in Fig. 3(f). The cholesterol unit cell determined from the diffraction data in Fig. 3(c) is indicative of a doubling of the lipid tail unit cell for the cholesterol molecules. The corresponding cholesterol structure consists of cholesterol pairs alternating between two different orientations.

The l_d-and the l_o-type structures can be related to the well-known umbrella model [48], where one lipid molecule is assumed to be capable to "host" two cholesterol molecules, which leads to a maximum cholesterol solubility of 66 mol% in saturated lipid bilayers. In this scenario the term umbrella model refers to two cholesterol molecules closely interacting with one lipid molecule. Cholesterol plaques, i.e., cholesterol bilayers coexisting with the lamellar membrane phase, were reported recently by Barrett *et al.* [33] in model membranes containing high amounts of cholesterol, above 40 mol% for DMPC and 37.5 mol% for DPPC. The triclinic peaks in Fig. 3(d) agree well with the structures published and were, therefore, assigned to cholesterol plaques.

Hence both coarse-grained molecular simulations and neutron diffraction data suggest the coexistence of a liquid disordered membrane with two types of highly ordered cholesterol structures: One with some lipid content [Fig. 3(f)], corresponding to the first shoulder in the density histogram at $\mu = 7.8 k_B T$ [Fig. 2(a), inset], and one almost exclusively made of cholesterol [Fig. 3(g)], corresponding to the second peak at $\mu = 7.8 k_B T$ in Fig. 2(a). The existence of these structures in the experiment should be robust in binary systems and not depend on, for instance, the sample preparation protocol [49].

The neutron diffraction data present evidence for pairs of strongly bound cholesterol molecules. We note that the scattering experiment was not sensitive to *single* cholesterol molecules; however, the formation of cholesterol dimers with a well-defined nearest neighbor distance leads to a corresponding peak in the data in Figs. 3(c) and 3(d). An attractive force between cholesterol molecules in a 1-palmitoyl-2-oleoylphosphatidylcholine (POPC) bilayer and the formation of cholesterol dimers was reported from MD simulations [50]. Such a force is likely related to the formation of lipid-cholesterol complexes [51] and the umbrella model. However, it is not straightforward to estimate the percentage of dimers from the experiments. A dynamical equilibrium between dimers and monomers is a likely scenario [52].

The dynamic domains observed in this study are not biological rafts, which are thought to be more complex, multi-component structures in biological membranes. In the past, domains have been observed in simple model systems, but only those designed to be "raft-forming" mixtures. In these cases the domains that form are stable equilibrium structures, and are not likely related to the rafts that exist in real cells [12]. The small and fluctuating domains observed in binary systems may be more closely related to what rafts are thought to be [10], and are potentially the nuclei that lead to the formation of rafts in biological membranes. The characteristic overall length scale for nanodomains in the simulations is around 20σ, corresponding to 10–20 nanometers. Both simulations and experiments indicate that there are two types of cholesterol-rich patches coexisting with cholesterol-poor liquid-disordered regions, i.e., ordered l_o-type regions containing both lipids and cholesterol, and cholesterol plaques. The transition between these two is gradual in the coarse-grained simulations. In real membranes, they have different

TABLE I. Peak parameters of the correlation peaks observed in Figs. 3(c) and 3(d) and the association with the different cholesterol structures, such as l_d-, l_o-type structure and cholesterol plaque. H and C label the nearest neighbor distances of lipid head groups and cholesterol molecules, respectively; T_1, T_2, and T_3 denote the unit cell of the lipid tails in the l_d regions of the membrane. Peaks were fitted using Gaussian peak profiles and widths are listed as Gaussian widths, σ_G.

	Amplitude (counts)	Center (Å^{-1})	σ_G (Å^{-1})	l_d	monoclinic cholesterol l_o-type structure	triclinic cholesterol plaque
Fig. 3(c)	62	0.75	0.17	H		
	117	1.360	0.46	T_1		
	27.5	1.360	0.17	C		
	46.6	2.289	0.05	T_2		
	15.0	2.650	0.10	T_3		
Fig. 3(d)	19.8	0.5	0.01			[1 0 0]
	34.8	0.55	0.01		[1 $\bar{1}$ 0]	
	34.3	0.74	0.01		[1 0 0]	[1 1 0]
	33.5	0.98	0.01			[2 0 0]
	110	1.12	0.01		[2 $\bar{1}$ 0]	
	117.8	1.32	0.01		[1 1 0]	
	60.0	1.61	0.01			[1 3 0]

local structures (monoclinic in l_o-type regions, triclinic in plaque regions), which may stabilize distinct domains.

This work was supported by the German Science Foundation within the collaborative research center SFB-625. Simulations were carried out at the John von Neumann Institute for Computing (NIC) Jülich and the Mogon Cluster at Mainz University. Experiments were funded by the Natural Sciences and Engineering Research Council (NSERC) of Canada, the National Research Council (NRC), the Canada Foundation for Innovation (CFI), and the Ontario Ministry of Economic Development and Innovation. L. T. is the recipient of an NSERC Canada Graduate Scholarship; M. C. R. is the recipient of an Early Researcher Award from the Province of Ontario.

*Corresponding author.
rheinstadter@mcmaster.ca
†friederike.schmid@uni-mainz.de

[1] K. Simons and E. Ikonen, Nature (London) **387**, 569 (1997).
[2] K. Simons and E. Ikonen, Science **290**, 1721 (2000).
[3] D. M. Engelman, Nature (London) **438**, 578 (2005).
[4] P. S. Niemelä, S. Ollila, M. T. Hyvönen, M. Karttunen, and I. Vattulainen, PLoS Comput. Biol. **3**, e34 (2007).
[5] L. J. Pike, J. Lipid Res. **50**, S323 (2009).
[6] D. Lingwood and K. Simons, Science **327**, 46 (2010).
[7] C. Eggeling, C. Ringemann, R. Medda, G. Schwarzmann, K. Sandhoff, S. Polyakova, V. N. Belov, B. Hein, C. von Middendorf, A. Schönle, and S. W. Hell, Nature (London) **457**, 1159 (2009).
[8] F. G. van der Goot and T. Harder, Seminars in immunology **13**, 89 (2001).
[9] P.-F. Lenne and A. Nicolas, Soft Matter **5**, 2841 (2009).
[10] K. Simons and M. J. Gerl, Nat. Rev. Mol. Cell Biol. **11**, 688 (2010).
[11] O. G. Mouritsen, Biochim. Biophys. Acta **1798**, 1286 (2010).
[12] M. C. Rheinstädter and O. G. Mouritsen, Curr. Opin. Colloid Interface Sci. **18**, 440 (2013).
[13] A. Dibble, A. K. Hinderliter, J. J. Sando, and R. L. Biltonen, Biophys. J. **71**, 1877 (1996).
[14] O. G. Mouritsen and R. L. Biltonen, New Compr. Biochem. **25**, 1 (1993).
[15] O. G. Mouritsen and K. Jørgensen, Chem. Phys. Lipids **73**, 3 (1994).
[16] O. G. Mouritsen and K. Jørgensen, Curr. Opin. Struct. Biol. **7**, 518 (1997).
[17] D. Marsh, Biochim. Biophys. Acta Biomembr. **1798**, 688 (2010).
[18] H. J. Risselada and S. J. Marrink, Proc. Natl. Acad. Sci. U.S.A. **105**, 17367 (2008).
[19] M. L. Berkowitz, Biochim. Biophys. Acta Biomembr. **1788**, 86 (2009).
[20] W. Bennett and D. P. Tieleman, Biochim. Biophys. Acta Biomembr. **1828**, 1765 (2013).
[21] F. A. Heberle, R. S. Petruzielo, J. Pan, P. Drazba, N. Kucerka, R. F. Standaert, G. W. Feigenson, and J. Katsaras, J. Am. Chem. Soc. **135**, 6853 (2013).
[22] S. Meinhardt, R. L. C. Vink, and F. Schmid, Proc. Natl. Acad. Sci. U.S.A. **110**, 4476 (2013).
[23] A. J. Sodt, M. L. Sandar, K. Gawrisch, R. W. Pastor, and E. Lyman, J. Am. Chem. Soc. **136**, 725 (2014).
[24] C. L. Armstrong, M. A. Barrett, A. Hiess, T. Salditt, J. Katsaras, A.-C. Shi, and M. C. Rheinstädter, Eur. Biophys. J. **41**, 901 (2012).
[25] C. L. Armstrong, D. Marquardt, H. Dies, N. Kučerka, Z. Yamani, T. A. Harroun, J. Katsaras, A.-C. Shi, and M. C. Rheinstädter, PLoS One **8**, e66162 (2013).
[26] C. L. Armstrong, W. Häußler, T. Seydel, J. Katsaras, and M. C. Rheinstädter, Soft Matter **10**, 2600 (2014).
[27] F. Schmid, D. Düchs, O. Lenz, and B. West, Comput. Phys. Commun. **177**, 168 (2007).
[28] B. West, F. L. H. Brown, and F. Schmid, Biophys. J. **96**, 101 (2009).
[29] G. Lindblom and G. Orädd, Biochim. Biophys. Acta **1788**, 234 (2009).
[30] A. H. de Vries, S. Yefimov, A. E. Mark, and S. J. Marrink, Proc. Natl. Acad. Sci. U.S.A. **102**, 5392 (2005).
[31] O. Lenz and F. Schmid, Phys. Rev. Lett. **98**, 058104 (2007).
[32] R. Vist and J. H. Davis, Biochemistry **29**, 451 (1990).
[33] M. Barrett, S. Zheng, L. Toppozini, R. Alsop, H. Dies, A. Wang, N. Jago, M. Moore, and M. Rheinstädter, Soft Matter **9**, 9342 (2013).
[34] See Supplemental Material at http://link.aps.org/supplemental/10.1103/PhysRevLett.113.228101 for details of molecular dynamics simulations and data analysis from the neutron scattering experiment, which includes Refs. [35–44].
[35] N. Chu, N. Kučerka, Y. Liu, S. Tristram-Nagle, and J. F. Nagle, Phys. Rev. E **71**, 041904 (2005).
[36] D. Frenkel and B. Smit, *Understanding Molecular Simulation: From Algorithms to Applications* (Academic, New York, 2001).
[37] L. Hosta-Rigau, Y. Zhang, M. T. Boon, A. Postma, and B. Städler, Nanoscale **5**, 89 (2012).
[38] J. Katsaras, R. F. Epand, and R. M. Epand, Phys. Rev. E **55**, 3751 (1997).
[39] O. Lenz and F. Schmid, J. Mol. Liq. **117**, 147 (2005).
[40] S. Mabrey and J. Sturtevant, Proc. Natl. Acad. Sci. U.S.A. **73**, 3862 (1976).
[41] W. D. Ness, Chem. Rev. **111**, 6423 (2011).
[42] H. Rauch, Found. Phys. **23**, 7 (1993).
[43] J. R. Taylor, *An Introduction to Error Analysis: The Study of Uncertainties in Physical Measurements* (University Science Books, Sausalito, 1982).
[44] A. Zheludev, "Reslib," http://www.neutron.ethz.ch/research/resources/reslib (2009).
[45] W. Witt, Z. Naturforschg. **22a**, 92 (1967).
[46] C. L. Armstrong, M. A. Barrett, L. Toppozini, N. Kučerka, Z. Yamani, J. Katsaras, G. Fragneto, and M. C. Rheinstädter, Soft Matter **8**, 4687 (2012).
[47] H. Rapaport, I. Kuzmenko, S. Lafont, K. Kjaer, P. B. Howes, J. Als-Nielsen, M. Lahav, and L. Leiserowitz, Biophys. J. **81**, 2729 (2001).
[48] J. Huang and G. W. Feigenson, Biophys. J. **76**, 2142 (1999).
[49] E. Elizondo, J. Larsen, N. S. Hatzakis, I. Cabrera, T. Børnholm, J. Veciana, D. Stamou, and N. Ventosa, J. Am. Chem. Soc. **134**, 1918 (2012).
[50] Y. Andoh, K. Oono, S. Okazaki, and I. Hatta, J. Chem. Phys. **136**, 155104 (2012).
[51] H. M. McConnell and A. Radhakrishnan, Biochim. Biophys. Acta Biomembr. **1610**, 159 (2003).
[52] J. Dai, M. Alwarawrah, and J. Huang, J. Phys. Chem. B **114**, 840 (2010).